ORIGINAL ARTICLE

Corneal Deformation Response with Dynamic Ultra-high-speed Scheimpflug Imaging for Detecting Ectatic Corneas

[1-3]Marcella Q Salomão, [2-6]Fernando F Correia, [2-7]Isaac Ramos, [1,2,8]Allan Luz, [1-3]Renato Ambrósio Jr

ABSTRACT

Purpose: To test the ability of metrics derived from corneal response to noncontact tonometry (NCT) to distinguish between normal and ectatic cases.

Materials and methods: The prototype of CorVis ST (Oculus, Wetzlar, Germany) was used for assessing corneal biomechanical response using ultra-high-speed 8 mm horizontal Scheimpflug photography, taking 4,330 frames per second during NCT. Patients were stratified based on clinical data, including rotating Scheimpflug corneal tomography (Oculus Pentacam HR). Biomechanical data from one eye randomly selected of 177 patients with normal corneas (N) and from 79 patients with bilateral keratoconus (KC) were investigated. Group forme fruste keratoconus (FFKC) was composed of 20 eyes with normal topographic patterns from cases with ectasia detected in the fellow eye. Group keratoconus suspect (KCS) had 16 eyes from 16 patients with topographic patterns suspicious of KC but documented stability over 3 years and normal tomographic findings. A combination of deformation parameters using linear regression analysis (Prototype Factor 1, pF1) was created by the BrAIn (Brazilian Artificial Intelligence on Corneal Tomography and Biomechanics) study group in order to provide the best possible separation of KC and normals.

Results: Statistical significant differences were found for N×KC for several parameters, including first and second applanation times, deformation amplitude, and maximal concavity radius (Mann–Whitney, $p < 0.001$). However, the areas under the receiver operating characteristic curves (AUC) were lower than 0.90. The pF1 had AUC of 0.945 (IC 0.909–0.97; sensitivity = 87.3% and specificity = 89.3%). The pF1 had statistically significant differences between the ectatic (KC and FFKC) and nonectatic groups (N and KCS) ($p < 0.05$, Kruskall–Wallis Test with *post hoc* Dunn's test).

Conclusion: Corneal deformation response analysis by ultra-high-speed 8 mm horizontal Scheimpflug photography provides relevant data for distinguishing ectatic and nonectatic corneas but cannot be used independently to detect KC. This data may be integrated with corneal tomography data for enhancing sensitivity and specificity for screening ectasia.

Keywords: Corneal biomechanics, CorVis ST, Forme fruste keratoconus, Keratoconus.

[1-8]Research Associate, [1-3]Associate Professor

[1]Department of Ophthalmology, Federal University of São Paulo, São Paulo, Brazil

[2]Rio de Janeiro Corneal Tomography and Biomechanics Study Group, Brazil

[3]Instituto de Olhos Renato Ambrósio and VisareRIO, Rio de Janeiro, Brazil

[4]Department of Cornea and Refractive, Hospital de Braga Braga, Portugal

[5]Department of Cornea and Refractive, Instituto CUF Porto Porto, Portugal

[6]School of Health Sciences, University of Minho, Braga, Portugal

[7]Hospital de Olhos Santa Luzia, Maceió, Brazil

[8]Hospital de Olhos de Sergipe, Aracaju, Brazil

Corresponding Author: Marcella Q Salomão, Department of Ophthalmology, Barra Vision Center, Rio de Janeiro, Brazil Phone: +552132825128, e-mail: marcella@barravisioncenter.com.br

INTRODUCTION

Keratoconus (KC) is an ectatic corneal dystrophy that has been described and studied for several decades.[1,2] There was considerable progress related to refractive surgery over the past three decades, which boosted significant improvements in the diagnosis and management of ectatic conditions.[3-5] Patients with ectatic disorders frequently present with subclinical disease as refractive surgery candidates. Such cases should be identified because these cases typically have unsatisfactory results and are at very high risk for progressive ectasia after laser vision correction (LVC).[6,7] Furthermore, the identification of early stages of the disease turned out to be indispensable considering new treatment modalities, such as corneal collagen cross-linking (CL).[8,9]

Since the first report of post-LASIK ectasia by Seiler in 1998, the concept of biomechanical decompensation caused by corneal ectasia was vented.[5,6] Hence, preventing ectasia is related to the identification of cases at a higher risk for biomechanical failure. Definitely, the advent and evolution of corneal topography[10,11] and tomography[12] enhanced our ability to detect these milder forms of ectatic diseases, with no clinical signs or visual acuity loss.[13] However, curvature and pachymetric changes

should probably be secondary events, while abnormalities in biomechanical properties and architecture stability should be expected primarily.[14]

The goal of this study was to test the ability of corneal biomechanical metrics derived from Dynamic Ultra High-Speed Scheimpflug Photography (the CorVis ST prototype) to distinguish normal from ectatic cases.

MATERIALS AND METHODS

This study adhered to the tenets of the Declaration of Helsinki. Patients from Instituto de Olhos Renato Ambrósio (Rio de Janeiro, Brazil) were retrospectively enrolled in the study. All eyes were examined by a fellowship-trained cornea and refractive surgeon (RA). Corneal biomechanics was assessed by the prototype of the Oculus CorVis ST (Oculus, Wetzlar, Germany), a new device with an ultra-high-speed 8 mm horizontal Scheimpflug camera that takes 4,330 frames per second during noncontact tonometry (NCT).

Along with a comprehensive ocular examination, all eyes were examined by a Placido-disk-based corneal topography (Atlas Corneal Topography System; Humphrey, San Leandro, California or Keratograph 4; Oculus, Wetzlar, Germany) and rotating Scheimpflug corneal tomography (Pentacam HR; Oculus, Wetzlar, Germany). Diagnosis of clinical KC was made based on Placido-disk-based axial topography, elevation-derived anterior corneal curvature maps, and criteria used in the collaborative longitudinal evaluation of KC.[15] Cases with a history of corneal surgery or with extensive corneal scarring were excluded from the study. Contact lens wearers were asked to discontinue the use at least 3 weeks prior to the examinations.

One eye randomly selected from 177 patients with topo- and tomographically comprised the normal corneas group (N). One eye randomly selected from 79 patients with bilateral KC comprised the KC group (group KC). Twenty eyes with normal topographic patterns from patients with clinical ectasia in the fellow eye were included in group forme fruste KC (FFKC). The keratoconus suspect (KCS) group comprised 16 eyes with topographic patterns suspicious of KC from 16 patients with documented stability over 3 years and normal tomography (Stable-KCS). We considered this as normal tomography if the eye had normal corneal thickness spatial profiles[16] along with normal anterior and posterior elevation values[17] and final D value.[18-20] The intraocular pressure, along with applanation and deformation responses, was extracted. The hypothesis on this study was that the non-ectatic groups (N and Stable-KCS) would have different deformation responses than groups with ectatic corneas (FFKC and KC groups).

Statistical analysis was accomplished using BioEstat 5.0 (Instituto Mamiraua, Amazonas, Brazil) and MedCalc 12.0 (MedCalc Software, Mariakerke, Belgium) according to Lopes et al.[21] The unpaired nonparametric Mann–Whitney test (Wilcoxon ranked-sum) was used to assess if the parameters have different distributions among N and KC. A p-value <0.05 was considered statistically significant. Receiver operating characteristic (ROC) curves were calculated for the parameters with significant differences to determine the test's overall predictive accuracy and area under the curve (AUC). A combined parameter using linear regression analysis (Prototype Factor 1, pF1) was created by the BrAIn (Brazilian Artificial Intelligence on Corneal Tomography and Biomechanics) study group in order to provide the best possible separation of KC and normals. The Kruskall–Wallis test with *post hoc* Dunn's test was used to test differences among the four groups (N, KCS, FFKC, and KC) for pF1.

RESULTS

There were no statistical differences for patient age or gender between the groups. Table 1 demonstrates computed corneal deformation metrics. Considering N and KC groups, statistically significant distributions were found for all studied parameters (Mann–Whitney, $p < 0.05$). However, there was a significant overlap that limits the diagnostic relevance. The best parameter was the radius of curvature at highest concavity, with an area

Table 1: Corneal deformation metrics

Parameter	Description
1st A Time	Moment at the first applanation of the cornea during the air puff (ms)
HC Time	Moment that the cornea assumes its maximum concavity during the air puff (ms)
2nd A Time	Moment at the second applanation of the cornea during the air puff (ms)
1st A Length (max)	The length of the applanation at the moment of the first applanation (mm)
2nd A Length (max)	The length of the applanation at the moment of the second applanation (mm)
Def.Amp. (max)	Measurement (mm) of the maximum corneal deformation during the air puff
W-Dist.	Length of the distance between the two peaks of the cornea at the moment of maximum deformation (mm)
Curv. Rad. HC	Corneal curvature radius at the time of maximum concavity during the air puff (mm)
Curv. Rad. Normal	Radius of curvature of the cornea in its natural state (mm)
V_{in}	Maximum velocity of the cornea during the ingoing phase (m/s)
V_{out}	Maximum velocity of the cornea during the outgoing phase (m/s)
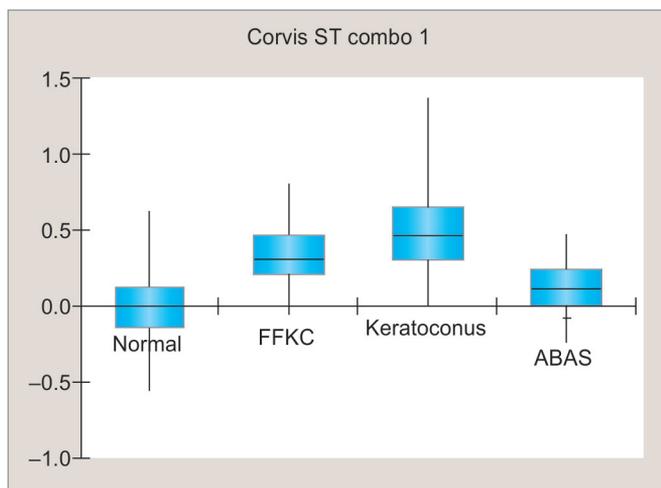
Graph 1: Area under the ROC curve of the radius of curvature at highest concavity
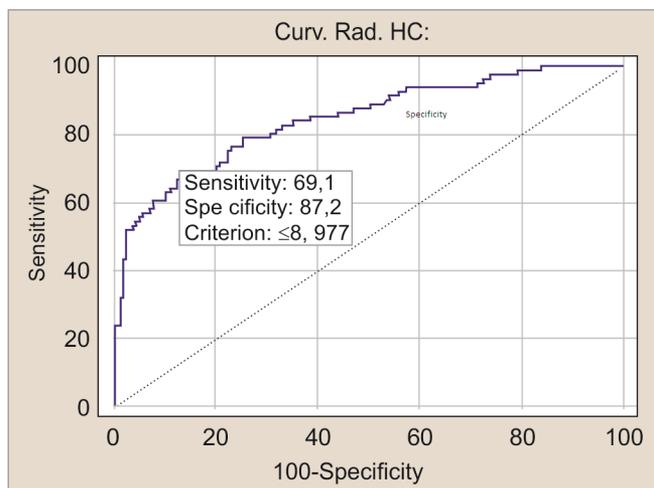

Graph 3: Box plots demonstrating average and standard deviation values in each group

Box 1: Corvis Factor 1 Formula

0.033* IOP - 0.004* Pachy Apex - 0.448* 1st A Time - 0.049* HC Time + 0.093* 2nd A Time + 0.026* 1st A Length(max) - 0.105* 2nd A Length(max) + 0.208* Def Amp (max) - 0.619* W-Dist - 0.021* Curv, Rad, HC-0.101* Curv, Rad, Normal - 0.525* V_{in} - 0.166* V_{out} + 7.952

Table 3: The post hoc Dunn's test found no differences between the FFKC and KC groups and N and KCS groups, but there were significant differences for N×FFKC, for N×KC, stable-KCS×FFKC and stable-KCS×KC

	Normal	KC	FFKC	ABT/IS
Normal		<0.05	<0.05	NS
KC			NS	<0.05
FFKC				<0.05
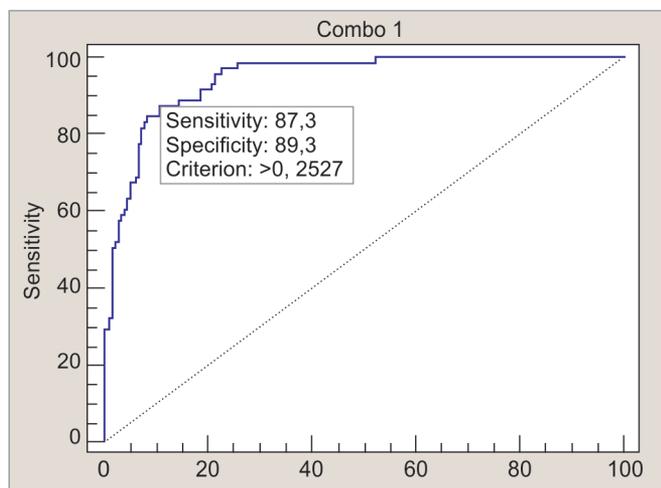
Graph 2: The combined parameter pF1 had AUC of 0.945

under the ROC curve of 0.845 (Graph 1). The combined parameter pF1 had AUC of 0.945 (Box 1 and Graph 2). Table 2 shows pF1 average and standard deviation values in each group and these data might also be appreciated in box plots on Graph 3. The distribution of pF1 was

Table 2: Corvis Factor 1 average and standard deviation values in each group

	N	FFK1	KC	ABT
Ave	−0.00801	0.345529	0.506829	0.133745
SD	0.218348	0.196043	0.26691	0.181624
	177	20	79	16

different among the groups (Kruskall–Wallis test). The *post hoc* Dunn's test found no differences between the FFKC and KC groups and N and KCS groups, but there were significant differences for N×FFKC, for N×KC, stable-KCS×FFKC, and stable-KCS×KC (Table 3).

DISCUSSION

Detecting milder forms of ectasia is fundamental for screening refractive surgery candidates[14] as well as for indicating less-invasive surgery (i.e., CXL and intracorneal ring implantation).[3] Iatrogenic ectasia is a rare complication after LVC, but due to the devastating nature of this complication, we must improve our understanding for prevention. Different studies have demonstrated the important role of corneal topography, tomography, and wavefront analysis in the screening of subclinical or mild ectatic disease.[22-24] Nevertheless, the hypothesis that focal biomechanical distress precedes topographic and tomographic alterations of the cornea is well accepted and prevails among experts. Hence, analyzing biomechanical properties of normal and subclinical KC eyes has gained special relevance.[25-28]

Biomechanical characterization is still challenging because of several biasing factors, such as the intraocular pressure and corneal thickness. While other noncontact tonometer, the Reichert ORA (Buffalo, NY, USA)

monitors corneal applanation response through the reflex of an infrared beam with diagnostic capability to detect ectasia,[29-31] ultra-high-speed Scheimpflug camera provides a dynamic visualization of the corneal deformation process with detailed information of the deformation response obtained during the NCT. A whole set of corneal deformation parameters is provided.[32,33] The Oculus CorVis ST imaging system is based on the instrument we used for this study and has been the subject of many studies in the characterization of corneal biomechanical properties.[34-36]

In this study, we analyzed *in vivo* corneal biomechanical properties from corneal deformation during NCT using the prototype of the CorVis ST. The relevance of this study is related to the ability to distinguish normal and ectatic corneas, even in early stages of the disease. While the data were not enough for solely identifying clinical KC, we identified a strong potential for the data derived from corneal deformation response to integrate with tomographic data in order to enhance sensibility and also specificity.

CONCLUSION

Corneal deformation response analysis by ultrahigh-speed 8 mm horizontal Scheimpflug photography provides relevant data for distinguishing ectatic and nonectatic corneas but cannot be used independently to detect keratoconus. This data may be integrated with corneal tomography data for enhancing sensitivity and specificity for screening ectasia.

REFERENCES

1. Krachmer JH, Feder RS, Belin MW. Keratoconus and related noninflammatory corneal thinning disorders. Surv Ophthalmol 1984 Jan-Feb;28(4):293-322.
2. Rabinowitz YS. Keratoconus. Surv Ophthalmol 1998 Jan-Feb; 42(4):297-319.
3. McGhee CN, Kim BZ, Wilson PJ. Contemporary treatment paradigms in keratoconus. Cornea 2015 Oct;34 (Suppl 10): S16-S23.
4. Renato A Jr. Keratoconus and ectatic corneal diseases: are we facing a new subspecialty? – Introduction. Int J Kerat Ect Cor Dis 2012;1(1):vii.
5. Gomes JA, Tan D, Rapuano CJ, Belin MW, Ambrósio R Jr, Guell JL, Malecaze F, Nishida K, Sangwan VS. Group of Panelists for the Global Delphi Panel of Keratoconus and Ectatic Diseases. Global consensus on keratoconus and ectatic diseases. Cornea 2015 Apr;34(4):359-369.
6. Seiler T, Quurke AW. Iatrogenic keratectasia after LASIK in a case of forme fruste keratoconus. J Cataract Refract Surg 1998 Jul;24(7):1007-1009.
7. Binder PS. Ectasia after laser in situ keratomileusis. J Cataract Refract Surg 2003 Dec;29(12):2419-2429.
8. Wollensak G, Spoerl E, Seiler T. Riboflavin/ultraviolet-a-induced collagen crosslinking for the treatment of keratoconus. Am J Ophthalmol 2003 May;135(5):620-627.
9. da Paz AC, Bersanetti PA, Salomao MQ, Ambrosio R Jr, Schor P. Theoretical basis, laboratory evidence, and clinical research of chemical surgery of the cornea: cross-linking. J Ophthalmol 2014;2014:890823.
10. Maeda N, Klyce SD, Tano Y. Detection and classification of mild irregular astigmatism in patients with good visual acuity. Surv Ophthalmol 1998 Jul-Aug;43(1):53-58.
11. Wilson SE, Ambrosio R. Computerized corneal topography and its importance to wavefront technology. Cornea 2001 Jul;20(5):441-454.
12. Ambrosio R Jr, Belin MW. Imaging of the cornea: topography *vs* tomography. J Refract Surg 2010 Nov;26(11):847-849.
13. Smadja D, Touboul D, Cohen A, Doveh E, Santhiago MR, Mello GR, Krueger RR, Colin J. Detection of subclinical keratoconus using an automated decision tree classification. Am J Ophthalmol 2013 Aug;156(2):237-246.e1.
14. Ambrosio R Jr, Randleman JB. Screening for ectasia risk: What are we screening for and how should we screen for it? J Refract Surg 2013 Apr;29(4):230-232.
15. Wagner H, Barr JT, Zadnik K. Collaborative longitudinal evaluation of keratoconus (clek) study: methods and findings to date. Cont Lens Anterior Eye 2007 Sep;30(4):223-232.
16. Ambrosio R Jr, Alonso RS, Luz A, Coca Velarde LG. Corneal-thickness spatial profile and corneal-volume distribution: tomographic indices to detect keratoconus. J Cataract Refract Surg 2006 Nov;32(11):1851-1859.
17. Belin MW, Khachikian SS. An introduction to understanding elevation-based topography: how elevation data are displayed – a review. Clin Exp Ophthalmol 2009 Jan;37(1):14-29.
18. Belin MW, Ambrosio R. Scheimpflug imaging for keratoconus and ectatic disease. Indian J Ophthalmol 2013 Aug;61(8):401-406.
19. Ambrosio R Jr, Valbon BF, Faria-Correia F, Ramos I, Luz A. Scheimpflug imaging for laser refractive surgery. Curr Opin Ophthalmol 2013 Jul;24(4):310-320.
20. Belin MW, Villavicencio OF, Ambrosio RR Jr. Tomographic parameters for the detection of keratoconus: suggestions for screening and treatment parameters. Eye Contact Lens 2014 Nov;40(6):326-330.
21. Lopes B, Ramos ICdO, Ribeiro G, Correa R, Valbon BdF, Luz ACd, Salomão M, Lyra JM, Ambrósio R Jr. Bioestatísticas: conceitos fundamentais e aplicações práticas. Rev Bras Oftalmol 2014;73(1):16-22.
22. Buhren J, Schaffeler T, Kohnen T. Validation of metrics for the detection of subclinical keratoconus in a new patient collective. J Cataract Refract Surg 2014 Feb;40(2):259-268.
23. Saad A, Gatinel D. Evaluation of total and corneal wavefront high order aberrations for the detection of forme fruste keratoconus. Invest Ophthalmol Vis Sci 2012 May 17;53(6):2978-2992.
24. Ambrosio R Jr, Ramos I, Lopes B, Santhiago MR, Faria-Correia F, Belin M, Binder PS. Ectasia susceptibility before laser vision correction. J Cataract Refract Surg 2015 Jun;41(6):1335-1336.
25. Luce DA. Determining *in vivo* biomechanical properties of the cornea with an ocular response analyzer. J Cataract Refract Surg 2005 Jan;31(1):156-162.
26. Luz A, Fontes BM, Lopes B, Ramos I, Schor P, Ambrósio R Jr. Ora waveform-derived biomechanical parameters to distinguish normal from keratoconic eyes. Arq Bras Oftalmol 2013 Mar-Apr;76(2):111-117.
27. Luz A, Fontes BM, Lopes B, Ramos I, Correia FF, Schor P, Ambrósio R Jr. Best waveform score for diagnosing keratoconus. Rev Bras Oftalmol 2013 Nov/Dec;72(6):361-365.

28. Ventura BV, Machado AP, Ambrosio R Jr, Ribeiro G, Araújo LN, Luz A, Lyra JM. Analysis of waveform-derived ora parameters in early forms of keratoconus and normal corneas. J Refract Surg 2013 Sep;29(9):637-643.

29. Fontes BM, Ambrosio R Jr, Jardim D, Velarde GC, Nose W. Ability of corneal biomechanical metrics and anterior segment data in the differentiation of keratoconus and healthy corneas. Arq Bras Oftalmol 2010 Jul-Aug;73(4):333-337.

30. Fontes BM, Ambrosio R Jr, Jardim D, Velarde GC, Nose W. Corneal biomechanical metrics and anterior segment parameters in mild keratoconus. Ophthalmology 2010 Apr; 117(4):673-679.

31. Luz A, Fontes BM, Lopes B, Ramos I, Schor P, Ambrosio R Jr. Ora waveform-derived biomechanical parameters to distinguish normal from keratoconic eyes. Arq Bras Oftalmol 2013 Mar-Apr;76(2):111-117.

32. Ambrósio R Jr, Ramos I, Luz A, Faria FC, Steinmueller A, Krug M, Belin MW, Roberts CJ. Dynamic ultra high speed scheimpflug imaging for assessing corneal biomechanical properties. Rev Bras Oftalmol 2013;72(2):99-102.

33. Koprowski R, Ambrosio R Jr, Reisdorf S. Scheimpflug camera in the quantitative assessment of reproducibility of high-speed corneal deformation during intraocular pressure measurement. J Biophotonics 2015 Nov;8(11-12):968-978.

34. Valbon BF, Ambrosio R Jr, Fontes BM, Luz A, Roberts CJ, Alves MR. Ocular biomechanical metrics by corvis st in healthy brazilian patients. J Refract Surg 2014 Jul;30(7):468-473.

35. Valbon BF, Ambrosio R Jr, Fontes BM, Alves MR. Effects of age on corneal deformation by non-contact tonometry integrated with an ultra-high-speed (uhs) scheimpflug camera. Arq Bras Oftalmol 2013 Jul-Aug;76(4):229-232.

36. Correia FF, Ramos I, Roberts CJ, Steinmueller A, Krug M, Ambrósio R Jr. Impact of chamber pressure and material properties on the deformation response of corneal models measured by dynamic ultra-high-speed scheimpflug imaging. Arq Bras Oftalmol 2013 Oct;76(5):278-281.